Symmetric and antisymmetric anisotropic exchange energies as crucial factors for the magnetic structures in Ho and Er

1992 J. Phys.: Condens. Matter 4 5735

(http://iopscience.iop.org/0953-8984/4/26/007)

J. Phys.: Condens. Matter 4 (1992) 5735–5745. Printed in the UK

Symmetric and antisymmetric anisotropic exchange energies as crucial factors for the magnetic structures in Ho and Er

J Sjöström
Department of Theoretical Physics, Royal Institute of Technology, S-100 44 Stockholm, Sweden

Received 14 October 1991

Abstract. The exchange energies for different magnetic phases in the heavy rare earths have been studied by means of an anisotropic band model. Calculations on Ho and Er show that the model predicts the correct magnetic ground states. The results show that the anisotropic rather than the isotropic exchange energy is crucial for the stability of competing magnetic structures. Particularly, in Er the strong spin–orbit coupling gives rise to an antisymmetric contribution to the anisotropic exchange energy. This antisymmetric contribution is a prerequisite for the conical configuration that takes place at low temperatures.

1. Introduction

The rare earths (RE) have, owing to their many remarkable magnetic properties, been the subject of many investigations; see Coqblin [1] for a survey.

Characteristic for the RE is the fact that the direction (helix) and the magnitude (modulation or spin-density wave (SDW)) of the magnetic moments may vary for crystallographically and chemically equivalent atoms. The variation can be described by one or several propagation vectors q, which can be commensurate or incommensurate with the period of the crystal. This means that superpositions of different spin configurations, for example a combination of a helix and ferromagnet constitute a conical structure in erbium and holmium, may obstruct the interpretation of the magnetic structure. In figure 1 we give a schematic survey of the magnetic phases and transition temperatures for heavy RE.

The physical reason for this complex magnetic behaviour can be traced back to the anisotropic exchange interaction [2–4] and the shape of the Fermi surface [5]. The latter property is called nesting, which means that the susceptibility has a peak for the spin propagation vector of the magnetic structure.

Traditionally, properties related to the electronic structure of the RE have been described by two contrasting methods: the band model and the crystal-field model. A band model with itinerant s, p and d electrons and the f electrons frozen in the core is used to describe the de Haas–van Alphen measurements, the transport properties, the crystal structure, etc. [1, 6]. In the crystal-field model, the f electrons play a central role, but it completely neglects the valence s, p and d electrons. That approach describes for example the magnetic moments and the LS coupling correctly [1, 6]. However, neither

0953-8984/92/265735 + 11 $04.50

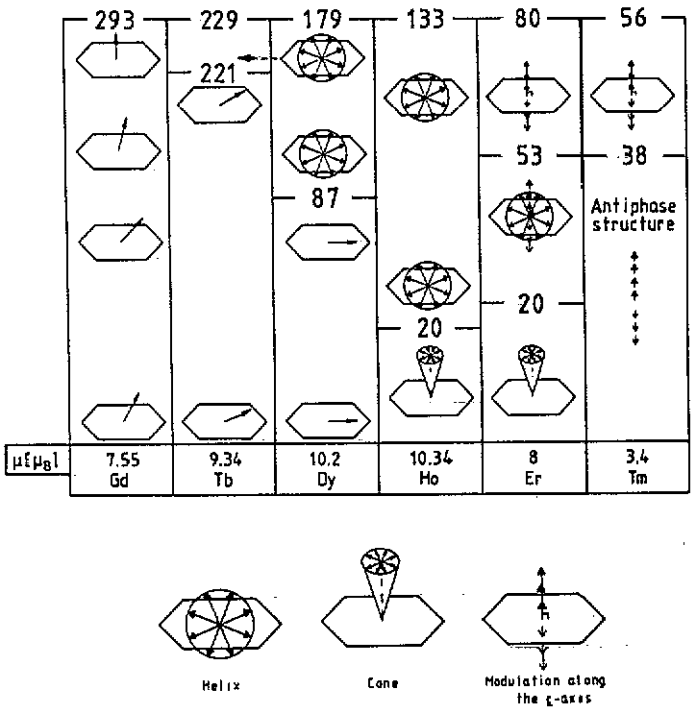

Figure 1. Magnetic structures, moments μ and transition temperatures for the heavy rare-earth elements (survey based on [1]).

model on its own can explain all the electronic properties. In fact, these models can be considered as two opposite and idealized special cases of the correct exchange interaction, which is of the so-called indirect type, i.e. an interaction between itinerant electrons and the magnetic moments from the localized f electrons [3].

A recently performed band calculation of Gd by Temmerman and Sterne [7] shows, however, that it is possible to include the f electrons with the traditional s, p and d valence electrons and in this way obtain reasonably accurate results for, e.g., the magnetic moments and the Fermi surface. This means that highly correlated f-electron systems can be based on a model where the exchange and correlation are derived from the electron-gas approximation. Calculations by Harmon [8] and Brooks *et al* [9] indicate that the band approach holds for the RE systems in general. Thus, it seems unambiguously that the correlated electron-gas approximation is relevant for the RE.

In an earlier work the author successfully applied a band model for the q-dependent susceptibility calculations on 3d systems with complex magnetic structures [10]. The purpose of this paper is to apply the same approach as in [10] and in this way study how different contributions to the exchange and band-structure properties influence the stability of competing magnetic structures in heavy RE. In section 5 we present results from numerical calculations for Ho and Er.

Finally we note that the spin susceptibility approach has recently been given a rigorous theoretical base for the RE [7–9, 11–13]. From a more pragmatic point of view, one knows, ever since the first paper by Liu *et al* in 1971 [5] (for calculations of, e.g., the spin propagation vector in erbium), that this approach is relevant for the RE.

2. Basic theory

In athe calculation of different contributions to the exchange energy we will use the anisotropic band model according to Sjöström [14]. It is based upon the approximation that the exchange interaction and spin–orbit interactions can be treated as perturbations of a non-magnetic Hamiltonian. This leads to a Hamiltonian that is not diagonal with respect to the spin–orbit term. Diagonalization results in an exchange energy and consequently also a susceptibility that depends on the orbital angular momentum vector, i.e. it is anisotropic. By assuming that the exchange can be described by a linear response theory function, and applying second-order perturbation theory, the following expression for the magnetic energy is obtained in [14]:

$$\varepsilon_{\mathrm{mag}}(\boldsymbol{q}) = \sum_{G,G'} \sum_{i,j} V_{\mathrm{ex},G} V^{*}_{\mathrm{ex},G'} S_{G,i}(\boldsymbol{q}) \chi^{-1}(\boldsymbol{q})_{GG',ij} S^{*}_{G',j}(\boldsymbol{q}). \tag{1}$$

Here $\boldsymbol{q}$ is the spin propagation wavevector, $V_{\mathrm{ex},G}$ and $S_{G,j}(\boldsymbol{q})$ are the Fourier components of the local exchange potential and the spin density. The latter is given by

$$S_{G,j}(\boldsymbol{q}) = (1/V) \int S(\boldsymbol{r}) \exp\{\mathrm{i}[\boldsymbol{q}_i \cdot (\boldsymbol{R}_n + \boldsymbol{\rho}) + \boldsymbol{\rho} \cdot \boldsymbol{G}]\} \, \mathrm{d}\boldsymbol{r}. \tag{2}$$

In the exchange field approximations (1) has the more handy form [10]

$$\varepsilon_{\mathrm{mag}}(\boldsymbol{q}) = \sum_{G,G'} \sum_{i,j} C_{GG'}(T) \langle S^{*}_{G,i}(\boldsymbol{q}) \rangle \chi_{GG',ij}(\boldsymbol{q}) \langle S_{G',j}(\boldsymbol{q}) \rangle. \tag{3}$$

Here the $\boldsymbol{q}$-independent constant $C_{GG'}(T)$ depends on $V_{\mathrm{ex},G}$ and on the magnetic transition temperature. Further, $\langle S_{G,i}(\boldsymbol{q}) \rangle$ is the mean value of the spins (defined in [10]) and the summations are over reciprocal lattice vectors $\boldsymbol{G}$, $\boldsymbol{G}'$ and space coordinate directions $(i, j = x, y, z)$.

The susceptibility tensor in (3) consists of two different contributions, one isotropic diagonal (χ^{IS}) term from the exchange interaction and one anisotropic. The latter thus has non-diagonal contributions, which arise from the exchange interaction and also indirectly from the spin–orbit interaction via the unitary diagonalization matrix U_K given in [14]. Thus we have

$$\chi(\boldsymbol{q})_{GG',ij} = \chi(\boldsymbol{q})^{\mathrm{IS}}_{GG'} \delta(i, j) + \chi(\boldsymbol{q})^{\mathrm{AN}}_{GG',ij}. \tag{4}$$

Here

$$\chi(\boldsymbol{q})^{\mathrm{IS}}_{GG'} = \sum_{k'} \sum_{k} F_G(k, k', k - q, k' + q) F_{G'}(k, k', k - q, k' + q)^{*} \times \frac{f(\varepsilon_{\mathrm{F}} - \varepsilon_k) f(\varepsilon_{\mathrm{F}} - \varepsilon_{k'}) f(\varepsilon_{k-q} - \varepsilon_{\mathrm{F}}) f(\varepsilon_{k'+q} - \varepsilon_{\mathrm{F}})}{\varepsilon_{k-q} + \varepsilon_{k'+q} - \varepsilon_k - \varepsilon_{k'}} \tag{5}$$

and

$$\chi(\boldsymbol{q})^{\mathrm{AN}}_{GG',ij} = \sum_{\substack{s,s',\\ s'',s'''}} \sum_{k,k'} \Lambda_{GG',ss's''s'''}(k, k', k - q, k' + q) \langle s''| U_{k-q} \sigma(1)_i U^{-1}_{k} |s\rangle \times \langle s| U_k \sigma(1)_j U^{-1}_{k-q} |s''\rangle \langle s'| U_{k'} \sigma(2)_i U^{-1}_{k'+q} |s'''\rangle \langle s'''| U_{k'+q} \sigma(2)_j U^{-1}_{k'} |s'\rangle \tag{6}$$

where

$$\Lambda_{GG',ss's''s'''}(k,k',k-q,k'+q) = (\mu_{\mathrm{B}}/\Omega) F_G(k,k',k-q,k'+q) F_G(k,k',k-q,k'+q)^{*} \times \left(\frac{f(\varepsilon_{\mathrm{F}} - \varepsilon_k + sL_k) f(\varepsilon_{\mathrm{F}} - \varepsilon_{k'} + s'L_{k'})}{\Delta\varepsilon + s''L_{k-q} + s'''L_{k'+q} - sL_k - s'L_{k'}} \right.$$

$$\times \frac{f(\varepsilon_{k-q} - s''L_{k-q} - \varepsilon_F) f(\varepsilon_{k'+q} - s'''L_{k'+q} - \varepsilon_F)}{\Delta\varepsilon + s''L_{k-q} + s'''L_{k'+q} - sL_k - s'L_{k'}}$$

$$- \frac{f(\varepsilon_F - \varepsilon_k) f(\varepsilon_F - \varepsilon_{k'}) f(\varepsilon_{k-q} - \varepsilon_F) f(\varepsilon_{k'+q} - \varepsilon_F)}{\Delta\varepsilon}\Bigg). \tag{7}$$

Here $F_G(k, k', k-q, k'+q)$ is the Fourier transform of the wavefunction, and $f(x)$ is the Fermi distribution function, i.e. $f(x) = 1$ for $x > 0$ and 0 for $x < 0$ when $T = 0$. Further ε_F is the Fermi energy, $\Delta\varepsilon = \varepsilon_{k-q} + \varepsilon_{k'+q} - \varepsilon_{k'} - \varepsilon_k$. In general the states k, k', $k-q$ and $k'+q$ belong to different bands. For brevity, however, the band indices have been suppressed in the expressions above. In (6), the summation is over all spin states that conserve the initial spins ($s + s' = s'' + s'''$).

The non-diagonal matrix elements of the susceptibility tensor (or its inverse) can be separated into a symmetric ($\chi^S_{\alpha\beta} = \chi^S_{\beta\alpha}$, $\alpha\beta = x, y, z$) and an antisymmetric term ($\chi^{AS}_{\alpha\beta} = -\chi^{AS}_{\beta\alpha}$). This means that the spin-dependent factors in the anisotropic energy expression (1) can also be separated into a symmetric and an antisymmetric term as follows [10]:

$$\varepsilon_{\alpha\beta} = (\chi^{-1}_{\alpha\beta})^S (S_{q\alpha}S^*_{q\beta} + S_{q\beta}S^*_{q\alpha}) + (\chi^{-1}_{\alpha\beta})^{AS} (S_{q\alpha}S^*_{q\beta} - S_{q\beta}s^*_{q\alpha}). \tag{8}$$

(For brevity q is here an index and G and G' are omitted.

In order to perform calculations of the anisotropic energy we need the explicit expressions of $(\chi_{\alpha\beta})^S$ and $(\chi_{\alpha\beta})^{AS}$ and they are given in appendix 1. We need also the Fourier transform for a general spin density

$$S(R_n + \rho)_\alpha = \sum_G \sum_q S_{G,\alpha}(q) \exp\{i[q \cdot (R_n + \rho) + \rho \cdot G]\} \tag{9}$$

where ρ is a distance vector in the unit cell n.

We note that relation (9) holds in the interesting special case of perfectly localized spins, i.e. if

$$S(\rho) = S\delta(\rho). \tag{10}$$

From (2) we get the corresponding Fourier components

$$S_G = S/V \tag{11}$$

which inserted in (9) gives the whole set of localized spins in the lattice

$$S(\rho) = S \sum_n \delta(R_n + \rho). \tag{12}$$

From the current magnetic structure we consider the following form of (9):

$$S(R_n + \rho)_\alpha = \sum_G \sum_q [S^H_{G,\alpha}(q_n) + S^{SDW}_{G,\alpha}(q_m)] \exp\{i[q \cdot (R_n + \rho) + \rho \cdot G]\}$$

$$= \sum_G \sum_q [a_n(u + iv) \exp[i\Phi(q_n)] \cdot$$

$$+ b_m w \sin(q_m \cdot r + \phi_m)] \exp\{i[q_m \cdot (R_m + \rho) + \rho \cdot G]\}. \tag{13}$$

Here H stands for a helix, a_n and b_m are constants and u, v, w are normalized vectors, directed in such a way that v and u are orthogonal to each other. Further in (13) $\Phi(q) = r \cdot q + \phi_0$ (ϕ_0 is the reference phase angle).

The expression (13) covers e.g. the following magnetic structures:

(i) Helix, $\Sigma_n a_n = 1$ and $b_m = 0$, $q_n \neq 0$.
(ii) SDW, $a_n = 0$ and $\Sigma_m b_m = 1$, $q_m \neq 0$.
(iii) Cone, $a_n \neq 0$, $b_m \neq 0$, $\Sigma_{n,m}(a_n + b_m) = 1$; u, v and w orthogonal; $q_n \neq 0$ and $q_m = 0$.
(iv) Modulations and bunching, $a_n \neq 0$, $b_m \neq 0$; w is parallel to the uv plane; $q_n \neq 0$ and $q_m \neq 0$.

3. General expressions for the symmetric and antisymmetric spin susceptibility in HCP rare earths

For the appropriate systems we consider the following different magnetic structures:

(i) Ferromagnetism in the *ab* plane or along the *c* axis.
(ii) Helix structure in the *ab* plane.
(iii) SDW along the *c* axis (or sinusoidal modulation).
(iv) Cone structure, i.e. superposition of (i) (with *z* as symmetry axis) and (ii).
(v) HSDW (helical SDW), i.e. a superposition of (ii) and (iii).

In the magnetic phase diagrams for the heavy RE, two or three of the spin arrangements above take place (depicted in figure 1). The transition between the different phases has been reproduced in mean-field theory by the *ad hoc* introduction of an anisotropic exchange field [4]. This indicates that the symmetric (SEI) and antisymmetric exchange interactions (AEI), which are physical bases for the anisotropic mean field, can be crucial factors for the stability of the magnetic structure.

In order to test this hypothesis we use the general expressions for the SEI and the AEI given in appendix 1 and the energy expression (3). We utilize also that the dispersion relation of L_k is simpler than for transition metals since, as a consequence of the localized interaction, the angular momenta obey Hund's rule for LS coupling. For the heavy elements this means that L and S are parallel and $J = L + S$.

In appendix 2, the following expressions are obtained.

(i) *Ferromagnetism*

$$\mathrm{SEI}_{GG'}(0) = \chi^{\mathrm{S}}_{GG',ii}(0) = 2\Lambda^{\mathrm{TOT}}(0) \tag{14a}$$

$$\mathrm{AEI}_{GG'}(0) = 0 \tag{14b}$$

($i = x, y$ or z) where

$$\Lambda^{\mathrm{TOT}}_{GG'}(0) = \sum_{s'',s'''} \sum_{s,s'} \Lambda_{GG',ss's''s'''}(k, k', k - q, k' + q) \qquad \text{for } q = 0.$$

The introduction of a q-dependent part of the symmetric SEI(q) and antisymmetric AEI(q) exchange energy is motivated in appendix 2.

(ii) *Helimagnetism*

$$\mathrm{SEI}_{GG'}(q_{\mathrm{h}}) = \Lambda^{\mathrm{TOT}}(q_{\mathrm{h}})[5 - 3\cos^2(q_{\mathrm{h}} \cdot R)]\cos(q_{\mathrm{h}} \cdot R) \tag{15a}$$

$$\mathrm{AEI}_{GG'}(q_{\mathrm{h}}) = 0. \tag{15b}$$

(iii) *Spin-density wave*

$$\mathrm{SEI}_{GG'}(\boldsymbol{q}_s) = 2\Lambda^{\mathrm{TOT}}(\boldsymbol{q}_s)\sin(\boldsymbol{q}_s \cdot \boldsymbol{R} + \alpha) \tag{16a}$$

$$\mathrm{AEI}_{GG'}(\boldsymbol{q}_s) = 0. \tag{16b}$$

(iv) *Cone structure*

$$\mathrm{SEI}_{GG'}(0, \boldsymbol{q}_c) = 2(\mu_z/\mu)^2\Lambda^{\mathrm{TOT}}_{GG'}(0) + (\mu_{xy}/\mu)^2\Lambda^{\mathrm{TOT}}_{GG'}(\boldsymbol{q}_c) \times [5 - 3\cos^2(\boldsymbol{q}_c \cdot \boldsymbol{R})]\cos(\boldsymbol{q}_c \cdot \boldsymbol{R}) \tag{17a}$$

$$\mathrm{AEI}_{GG'}(0, \boldsymbol{q}_c) = 4(\mu_z/\mu)^2\Lambda^{\mathrm{As}}_{GG'}(\boldsymbol{q}_c)\sin(\boldsymbol{q}_c \cdot \boldsymbol{R}) \tag{17b}$$

where

$$\Lambda^{\mathrm{As}}_{GG'}(\boldsymbol{q}_s, \boldsymbol{q}_h) = \Lambda_{GG',1-1-11}(\boldsymbol{k}, \boldsymbol{k}', \boldsymbol{k} - \boldsymbol{q}, \boldsymbol{k}' + \boldsymbol{q}) + \Lambda_{GG',-11-11}(\boldsymbol{k}, \boldsymbol{k}', \boldsymbol{k} - \boldsymbol{q}, \boldsymbol{k}' + \boldsymbol{q}).$$

(v) HSDW, i.e. a superposition of (ii) and (iii)

$$\mathrm{SEI}_{GG'}(\boldsymbol{q}_s, \boldsymbol{q}_h) = 2(\mu_z/\mu)^2\Lambda^{\mathrm{TOT}}_{GG'}(\boldsymbol{q}_s)\sin(\boldsymbol{q}_s \cdot \boldsymbol{R}) + (\mu_{xy}/\mu)^2\Lambda^{\mathrm{TOT}}_{GG'}(\boldsymbol{q}_h) \times [5 - 3\cos^2(\boldsymbol{q}_h \cdot \boldsymbol{R})]\cos(\boldsymbol{q}_h \cdot \boldsymbol{R}) \tag{18a}$$

$$\mathrm{AEI}_{GG'}(\boldsymbol{q}_h) = 4(\mu_z/\mu)^2\Lambda^{\mathrm{As}}_{GG'}(\boldsymbol{q}_h)\sin(\boldsymbol{q}_h \cdot \boldsymbol{R}). \tag{18b}$$

By determining the boundary conditions for expressions (15)–(18), we find that they are consistent with (14) in the time of $\boldsymbol{q} \to 0$.

4. Technical details in the calculations

The calculation procedure of the symmetric and antisymmetric contributions to the energy involves calculations of: (i) the energy bands, (ii) the susceptibilities (from (A1.1) and (A1.2)), (iii) the SEI and AEI according to the formulae in the previous section and (iv) the energies from (A2.2*a*) and (A2.2*b*).

(i) The band-structure calculations were performed using a self-consistent linear muffin-tin orbital (LMTO) method. Relativistic effects are included except for the spin–orbit interaction of the band electrons. This means that band splitting effects from the spin–spin and the spin–orbit interactions are taken into consideration only by perturbation calculations, i.e. not self-consistently. For the generation of the potential, the local-density approximation with Gunnarsson–Lundqvist parametrization was adopted. The calculations were made for the equilibrium hexagonal structure and with 3672 $\boldsymbol{k}$-points in the irreducible wedge of the Brillouin zone.

(ii) The following method and approximations have been used. We have considered only energy bands that cross the Fermi level in such a way that so-called nesting effects in principle are possible. Among these bands the different combinations of two-band systems have been selected. Inter- as well as intra-band interactions have been taken into account, while excitations involving more than two bands have been neglected. The summations over $\boldsymbol{k}$ and $\boldsymbol{k}'$ are performed over the same $\boldsymbol{k}$-mesh of the irreducible part of the Brillouin zone as for the band calculation. The $\boldsymbol{q}$-vectors of the helix have been set equal to that $\boldsymbol{k}$-point which deviates least from the experimental one, i.e. no interpolation between the $\boldsymbol{k}$-points was performed.

Step (iii) above was performed by using experimental results (given in [1] and the references in [1]) of the magnetic structures (mainly $\boldsymbol{q}$-vectors). For cases where hypothetical magnetic structures are investigated, we use values for $\boldsymbol{q}$-vectors, magnetic moments, etc., corresponding to the experimental values.

Table 1. The various contributions to the calculated exchange energy (meV) for the magnetic structures in section 3. Abbreviations: SAE = symmetric anisotropic exchange energy, AAE = antisymmetric anisotropic exchange energy, AE = total anisotropic exchange energy, IE = isotropic exchange energy and $\Delta\varepsilon$ = total energy difference relative to the experimental ground state. The numerical inaccuracy for the energy differences is estimated to be ±5 meV between ferromagnetism and the other structures, < ±1 between the cone and the HSDW or the helix (lower because the susceptibilities are calculated for the same q-vector). The absolute values have much larger inaccuracy.

		SAE (meV)	AAE (meV)	AE (meV)	IE (meV)	$\Delta\varepsilon$ (meV)
Ho	Ferrom.	−35	0	−35	−385	9
	Helix	−43.2	0	−43.2	−392	0.9
	SDW	−31	0	−31	−392	13
	Cone	42.8	−1.3	−44.1	−392	0
	HSDW	−42.1	−1.3	43.4	−392	0.7
Er	Ferrom.	−34	0	−34	−374	19
	Helix	−47	0	−47	−378	2
	SDW	−28	0	−28	−378	21
	Cone	−30	−19	−49	−378	0
	HSDW	−24	−19	−43	−378	6

Step (iv) involves the Fourier transforms of the electrostatic potential and the spins.

The crucial point is step (ii), i.e. the self-energy represented by the $\Lambda(\boldsymbol{q}_h)_{GG',ss's''s'''}$ in (A1.1) and (A1.2), because they involve energy differences in the denominators, which can be very small. We have approached this problem by using a much finer mesh in the $\boldsymbol{k}$-space than for ordinary band calculations. In this way we obtain high convergence for the Fermi level and the energy bands. It is important to note that the uncertainty in step (ii) primarily deteriorates the absolute values but also as a secondary effect the energy differences between ferromagnetism and the non-collinear structures but not the energy differences between structures corresponding to the same q-vector and matrix elements. The numerical accuracy of the energy differences is, as a consequence of this cancellation of the systematic errors of the subtraction in (A1.1) and (A1.2), high (table 1). Of course, we have not taken into consideration the errors from the approximation involved in the method (since they are impossible to estimate).

5. Computational study on Ho and Er

In this section we apply the computational method described in section 4 on Er and Ho.

We utilize the following experimental data. Between T_N = 88 K and T_c = 20 K the magnetic structure of Ho is a basal plane helix, which transfers to a cone structure [15] (type (iv)). Er also has a cone structure in the ground state but the semi-cone angle is less than for Ho (30° and 80.5°) [1, 15, 16]. The different cone angles are a consequence of the fact that the b axis is the easy magnetization direction in Ho while in erbium the easy axis is the c axis. The helix in Ho is distorted by the anisotropy in such a way that the moment is bunched around the easy axis [17]. The high-temperature structure in Er is a SDW, which propagates along the hexagonal c axis. The intermediate phase is a superposition of a helix and a SDW, i.e. structure (v) above.

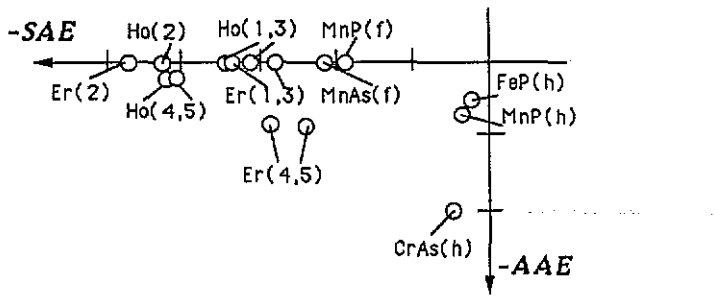

Figure 2. Schematic illustration of the results from the computational studies of the symmetric (SAE) and the antisymmetric (AAE) contributions to the anisotropic exchange energy in the different magnetic phases in MnP, FeP, CrAs, MnAs [10], Ho and Er. For the transitions metals, h stands for helix and f for ferromagnetism. For Ho and Er the element numbers correspond to a certain magnetic structure according to the list in section 4. The distance between two scale marks corresponds to 10 meV.

The result from the calculations is presented in table 1. It turns out that both Ho and Er get their lowest energy for the cone structure. This result in Er is a consequence of the fact that the cone structure, due to strong spin–orbit coupling, corresponds to a rather large AEI. The helical spin configuration has lower SEI than the cone structure but for a symmetry reason the AEI vanishes. It is interesting to note that the experimental value of the q-vector in Ho and Er is approximately coincident with the one for the lowest possible SEI for a helix (see appendix 2).

In Ho the AEI is small but nevertheless it tipped the scales in favour of the cone structure. For Er the results obtained are significant within the numerical inaccuracy. This is probably the case even for Ho since the dominating element is calculated for the same q-vector.

Nesting effects (section 1) occur in both Er and Ho (table 1), but in this calculation isotropic nesting is obviously not the determining factor.

The magnitudes of the total anisotropic energy are about 13% in Er and 11% in Ho at the total exchange energy.

In figure 2, the SEI and AEI for Ho and Er are compared with the same quantities for MnP, FeP, CrAs and MnAs in [10].

6. Discussion

We have shown in figure 2 that the AEI and SEI for a number of magnetic systems vary with the magnetic structure. Since the isotropic exchange interaction is not directionally dependent, it is clear that the stability of competing magnetic structures is governed not only by the magnitude of the anisotropy, but also to a high degree by the ratio between its symmetric and antisymmetric contributions.

In fact there are two different problems concerning the stability of complex mangetic structures: (i) what is the value of $q_1, q_2, \ldots, q_N$; (ii) which spatial spin distribution corresponds to the lowest energy?

Contrary to the first problem, the second has not attracted so much attention. This work indicates that problem (ii) can be approached by taking the SEI and AEI into consideration. This can also be done experimentally, as Kataoka has noticed [18],

by study the dynamical spin–wave spectra. The spin distribution can be measured by neutron diffraction, Mössbauer spectroscopy or nuclear magnetic resonance (NMR). By combining these methods, the experimental resolution can be improved. A way to proceed on the theoretical side is to extend this computational work, e.g. by including the spin–orbit coupling for the band electrons and particularly by interpolation of the energy bands in k-space for the $\chi(q)$ calculation.

Appendix 1. Explicit expressions for the anisotropic susceptibility tensor

In [14], The non-diagonal susceptibility in equation (4) is separated into an antisymmetric (AS) and a symmetric term (S) in the following way:

$$\chi^{AS}_{GG',ij}(q) = iA(i,j)\Big[\sum_{\text{bands}}\sum_{\substack{s,s'\\ s'',s'''}}(\Lambda_{GG',1-1-11}+\Lambda_{GG',-11-11})(L_{(k-q)n}/L_{k-q}+L_{(k)n}/L_k)$$
$$\times(L_{(k'+q)n}/L_{k'+q}+L_{(k')n}/L_{k'})+\sum_{\text{bands}}\sum_{\substack{s,s'\\ s'',s'''}}(\Lambda_{GG',1111}+\Lambda_{GG',-1-1-1-1})$$
$$\times(L_{(k-q)n}/L_{k-q}-L_{(k)n}/L_k)(L_{(k'+q)n}/L_{k'+q}-L_{(k')n}/L_{k'})\Big] \qquad \text{(A1.1)}$$

and

$$\chi^{S}_{GG',ij}(q) = \sum_{\text{bands}}\sum_{\substack{s,s'\\ s'',s'''}}(\Lambda_{GG',1111}+\Lambda_{GG',-1-1-1-1}+\Lambda_{GG',1-1-11}+\Lambda_{GG',-11-11})$$
$$\times\Bigg(\delta(i,j)+\frac{L_{ki}L_{k'j}L_{(k-q)i}L_{(k'+q)j}}{L_kL_{k'}L_{k-q}L_{k'+q}}$$
$$+\frac{L_{kj}L_{k'i}L_{(k-q)j}L_{(k'+q)i}-(L_{k-q}\cdot L_k)(L_{k'+q}\cdot L_{k'})\delta(i,j)}{L_kL_{k'}L_{k-q}L_{k'+q}}\Bigg). \qquad \text{(A1.2)}$$

Here, i, j, n are space coordinate indices x, y or z, $\Lambda_{GG',ss's''s'''}$ is given in expression (7), and $A(i,j)$ is the antisymmetric tensor ($A(i,j)=1$, $A(j,i)=-1$ and $A(i,i)=0$). Note also that the n coordinate in (A1.2) is directed perpendicular to the spins. It is therefore obvious that the AEI vanishes if the n component of $L_k = 0$.

Appendix 2. Derivation of the symmetric and antisymmetric exchange energy in heavy rare earths

By inserting the susceptibility, given by expressions (A1.1) and (A1.2) for the magnetic structures labelled (i)–(v) in section 3, in the energy expression (3) we obtain the symmetric and antisymmetric contributions to the exchange energy. Besides the spin directions we also use that the angular momenta are parallel to the spins. Furthermore both S and L can as a good approximation be considered as localized.

For the ferromagnetic structure (i) only the direction that coincides with the spins survives:

$$\mathrm{SEI}_{GG'}(0) = \chi^{\mathrm{S}}_{GG',ii}(0) = 2\Lambda^{\mathrm{TOT}}_{GG'}(0) \tag{A2.1a}$$

$$\mathrm{AEI}_{GG'}(0) = 0 \tag{A2.1b}$$

($i = x, y$ or z) where

$$\Lambda^{\mathrm{TOT}}_{GG'}(0) = \sum_{s'',s'''} \sum_{s,s'} \Lambda_{GG',ss's''s'''}(k, k', k-q, k'+q) \qquad \text{for } q = 0.$$

The abbreviations $\mathrm{SEI}(q)$ and $\mathrm{AEI}(q)$ stand for the symmetric and antisymmetric terms of q-dependent part of the exchange energy [10], i.e.

$$\varepsilon_{\mathrm{SEI}}(q) = \sum_{G,G'} \mathrm{SEI}_{GG'}(q)\, C_{GG'}(T)\langle S_G\rangle\langle S^*_{G'}\rangle \tag{A2.2a}$$

$$\varepsilon_{\mathrm{AEI}}(q) = \sum_{G,G'} \mathrm{AEI}_{GG'}(q)\, C_{GG'}(T)\langle S_G\rangle\langle S^*_{G'}\rangle. \tag{A2.2b}$$

For a magnetic helix in the xy plane, i.e. structure (ii), we have four different contributions to SEI:

$$\mathrm{SEI}_{GG'}(q_{\mathrm{h}}) = [\chi^{\mathrm{S}}_{GG',xx}(q) + \chi^{\mathrm{S}}_{GG',yy}(q) + \chi^{\mathrm{S}}_{GG',xy}(q) + \chi^{\mathrm{S}}_{GG',yx}(q)]\cos(q_{\mathrm{h}} \cdot R). \tag{A2.3}$$

The last term on the right-hand side of (A2.3) comes from the scalar product between the reference spin and the first-nearest-neighbour (INN) (which of course rotates the angle $q_{\mathrm{h}} \cdot R$). This means that we have neglected terms of higher order than the second in the Fourier series expansions of all characters in (A2.2a) and (A2.2b).

If we choose the x direction as the reference spin direction, the yy component vanishes. Since the susceptibility is symmetric we simply add the xy and yx components. This yields

$$\mathrm{SEI}_{GG'}(q_{\mathrm{h}}) = [\chi^{\mathrm{S}}_{GG',xx}(q) + 2\chi^{\mathrm{S}}_{GG',xy}(q)]\cos(q_{\mathrm{h}} \cdot R). \tag{A2.4}$$

By using (A2.1) and (A2.3) we get for the INN and L_k parallel with a magnetic moment

$$\begin{aligned}\mathrm{SEI}_{GG'}(q_{\mathrm{h}}) &= \Lambda^{\mathrm{TOT}}_{GG'}(q_{\mathrm{h}})[3-\cos^2(q_{\mathrm{h}}\cdot R)]\cos(q_{\mathrm{h}}\cdot R) + 2\Lambda^{\mathrm{TOT}}_{GG'}(q_{\mathrm{h}})\sin^2(q_{\mathrm{h}}\cdot R)\cos(q_{\mathrm{h}}\cdot R) \\ &= \Lambda^{\mathrm{TOT}}_{GG'}(q_{\mathrm{h}})[3 - \cos^2(q_{\mathrm{h}} \cdot R) + 2\sin^2(q_{\mathrm{h}} \cdot R)]\cos(q_{\mathrm{h}} \cdot R) \\ &= \Lambda^{\mathrm{TOT}}_{GG'}(q_{\mathrm{h}})[5 - 3\cos^2(q_{\mathrm{h}} \cdot R)]\cos(q_{\mathrm{h}} \cdot R). \end{aligned} \tag{A2.5a}$$

This expression assumes it maximum for $\cos^2(q_{\mathrm{h}} \cdot R) = 5/9$, which corresponds to approximately 42°, i.e. close to experimental values for Ho and Er [15, 16]!

The antisymmetric contribution vanishes for the helix since $L_{k_2} = 0$,

$$\mathrm{AEI}_{GG'}(q_{\mathrm{h}}) = 0. \tag{A2.5b}$$

For the SDW (iii) all the spins are parallel and sinusoidal or modulated, so we get

$$\mathrm{SEI}_{GG'}(q_{\mathrm{s}}) = 2\Lambda^{\mathrm{TOT}}_{GG'}(q_{\mathrm{s}})\sin[(q_{\mathrm{s}} \cdot R) + \alpha] \tag{A2.6a}$$

$$\mathrm{AEI}_{GG'}(q_{\mathrm{s}}) = 0. \tag{A2.6b}$$

The cone structure is somewhat more complicated because it is a superposition of

the structures (i) and (ii). Moreover, the AEI term does not vanish since $L_{kz} \neq 0$. We write the symmetric term as

$$\mathrm{SEI}_{GG'}(q_s) = \mathrm{SEI}_{GG'}(0) \sin^2 \alpha + \mathrm{SEI}_{GG'}(q_c) \cos^2 \alpha. \tag{A2.7}$$

Here α is the semi-cone angle. Inserting (A2.1*a*) and (A2.5*a*) in (A2.7) and relating α to the magnetic moment we simply obtain the expression (17*a*) of $\mathrm{SEI}(q_c)$ given in section 3.

In order to calculate the antisymmetric term we used the following approximations. The (small) xz and zy components are neglected. The second product on the right-hand side of (A1.2) is put equal to zero, since it consists of terms that cancel to a large extent. We must also take into consideration that according to (8) the spins of the AEI term can be written as a vector product and consequently a sine term will appear. Within the framework of these approximations, it is straightforward to get expression (17*b*).

The HSDW is a superposition of a helix and and SDW. We obtain the AEI and the SEI in the same way as for the cone structure (expressions (18*a*) and (18*b*)).

References

[1] Coqblin B 1977 *The Electronic Structure of Rare-Earth Metals and Alloys* (London: Academic)
[2] Ruderman M A and Kittel C 1954 *Phys. Rev.* **96** 99
[3] Yosida K 1957 *Phys. Rev.* **106** 893
[4] Nagamiya T 1967 *Solid State Phys.* **20** (New York: Academic)
[5] Liu S H, Gupta R P and Sinha S K 1971 *Phys. Rev.* B **4** 1100
[6] Gshneidner and Eyring (ed) 1978 *Handbook on Physics and Chemistry of Rare Earths*
[7] Temmerman W M and Sterne P A 1990 *J. Phys.: Condens. Matter* **2** 5529
[8] Harmon B N 1979 *J. Physique Coll.* C **5** 65
[9] Brooks M, Nordström L and Johansson B 1991 *J. Phys.: Condens. Matter* **3** 2357
[10] Sjöström J 1992 *J. Phys.: Condens. Matter* **4** 5723
[11] Gupta R P and Freeman A 1976 *Phys. Rev.* B **13** 4376
[12] Yafet Y 1987 *J. Appl. Phys.* **61** 4058
[13] Majkrzak C F, Cable J M, Kwo J, Hong M, McWhang D B, Yafet Y and Waszczak J V 1986 *Phys. Rev. Lett.* **56** 2700
[14] Sjöström J 1990 *J. Phys.: Condens. Matter* **2** 4637
[15] Koehler W C, Cable J W, Child H R, Wilkensson M K and Wollan E O 1967 *Phys. Rev.* **158** 450
[16] Cable J W, Wollan E O, Koehler W C and Wilkensson M K 1965 *Phys. Rev.* A **140** 1896
[17] Koehler W C 1972 *Magnetic Properties of the Rare Earth Metals* (New York: Plenum) ch 3
[18] Kataoka M 1986 *J. Phys. Soc. Japan* **56** 3635